Computational Geosciences (2006) 10:179–200
DOI: 10.1007/s10596-005-9018-y

Probabilistic model for eruptions and associated flood events in the Katla caldera, Iceland

Jonas Eliasson[a], Gudrun Larsen[b], Magnus Tumi Gudmundsson[b] and Freysteinn Sigmundsson[c]

[a]*Engineering Research Institute, University of Iceland, Hjardarhaga 6, IS-107 Reykjavik, Iceland*
E-mail: jonase@hi.is
[b]*Institute of Earth Sciences, University of Iceland, Sturlugata 7, IS-101 Reykjavik, Iceland*
[c]*Nordic Volcanological Centre, Institute of Earth Sciences, Sturlugata 7, IS-101 Reykjavik, Iceland*

Accepted 8 August 2005

Eruptions in the subglacial Katla caldera, South Iceland, release catastrophic jokulhlaups (meltwater floods). The ice surface topography divides the caldera into three drainage sectors (Ko, So and En sectors) that drain onto Myrdalssandur, Solheimasandur and Markarfljot plains, respectively. In historical times, floods from the Ko sector have been dominant, with only two recorded So events. Geological records indicate that floods from the En sector occur every 500–800 years. A probabilistic model for an eruption is formulated in general terms by a stochastic parameter that simulates a series giving the time interval in years between two consecutive events. The model also contains a Markovian matrix that controls the location of the event and thereby what watercourse is hit by the flood. A record of Katla eruptions since the 8th and the 9th century A.D., and geological information of volcanogenic floods towards the west over the last 8,000 years is used to calibrate the model. The model is then used to find the probabilities for floods from the three sectors: Ko, So and En. The simulations predict that the most probable eruption interval for the En sector and the So sector is several times smaller than the average time interval, implying infrequent periods of high activity in these sectors. A correlation is found between the magnitude of eruptions and the following time intervals. Using the statistical approach and considering this magnitude–time interval correlation, the probability of an eruption in Katla volcano is considered to be 20% within the next 10 years. This compares to a probability of 93% if only a simple average is considered. These probabilities do not take account of long-term eruption precursors and should therefore be regarded as minimum values.

Keywords: Katla volcano, volcanic eruptions, jokulhlaups, catastrophic floods, probabilistic modeling, simulations, Markov processes, eruption probabilities.

1. Introduction

Katla is one of the most active volcanoes in Iceland. It is located near the south coast and the upper parts of the volcano are covered by the 600-km^2 Myrdalsjokull ice cap (figure 1). The ice cap conceals a large caldera, 100 km^2 in area, where the ice is 400–700 m thick [1]. South Iceland has a moist maritime climate with frequent rainfall, the annual precipitation at Myrdalsjokull is considered to be in excess of 4,000 mm/year. Thus, rivers draining the glacier and the neighbouring highlands frequently experience flooding related to high precipitation and/or rapid snowmelt in summer (e.g., [2]); flood discharge in the order of 500 m^3/s would be regarded as large for these rivers. These floods, however, are minuscule compared to the violent jokulhlaups caused by volcanic eruptions within the subglacial Katla caldera. These catastrophic jokulhlaups have flooded extensive areas to the east of the volcano about twice per century in the last 1,000 years, and repeatedly caused destruction and damage to property in the region (e.g., [3, 4]). In these jokulhlaups, several hundred km^2 of sandur plains have been flooded for several hours, and large volumes of sediments and ice blocks from the glaciers have been deposited on the Myrdalssandur plain to the southeast of the volcano (e.g., [5]).

The extent and depth of the Katla caldera was revealed by radio-echo soundings in 1991 [1], and it was shown that the caldera is divided into three water drainage basins, with meltwater from each basin draining out through a subglacial breach in the caldera wall (figures 1 and 2). This division of the caldera into drainage basins is caused by the ice surface topography, and not by intracaldera bedrock topography [1].

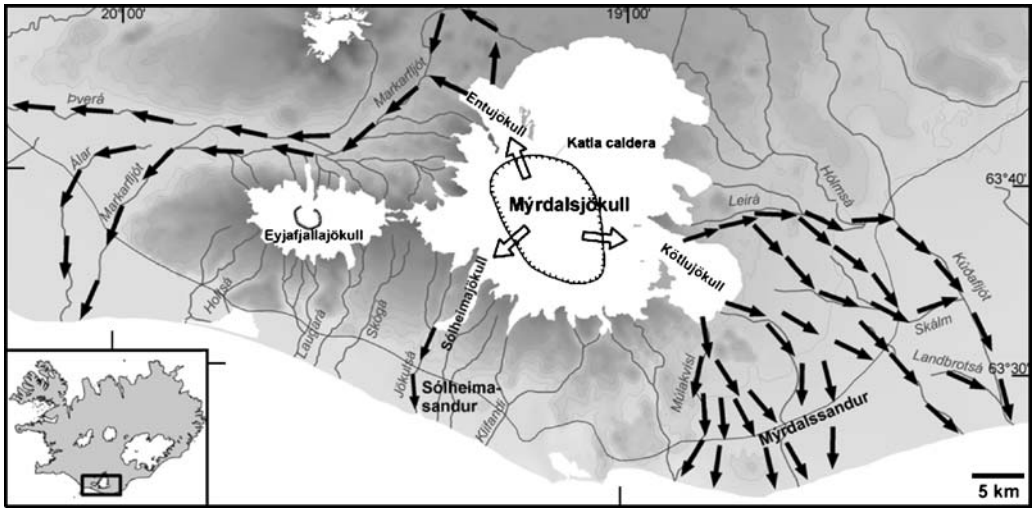

Figure 1. Myrdalsjokull glacier (white) and the surrounding area in South central Iceland. The hatched line indicates the rim of the Katla caldera. The filled arrows indicate main routes of jokulhlaups (glacial floods) while the white arrows through the caldera rim show the three subglacial outlets from the caldera [1].

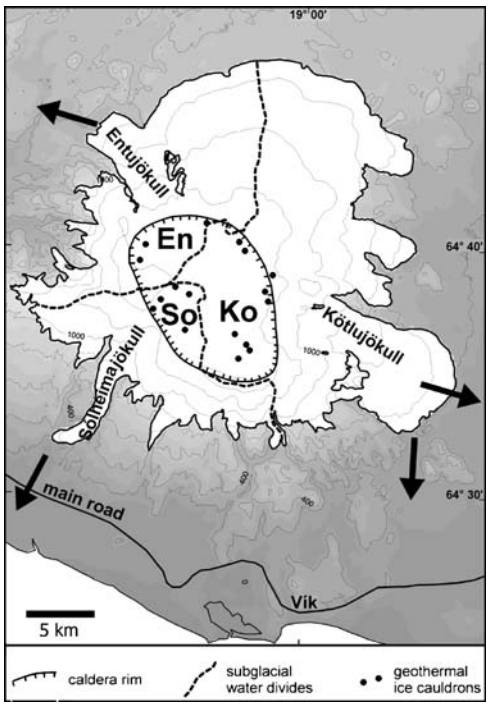

Figure 2. The Myrdalsjokull glacier, the Katla caldera, locations of geothermal activity within the caldera (ice cauldrons) and subglacial water divides [1]. The main routes of jokulhlaups from the three sectors (Ko, So, and En sectors) are shown with arrows.

The easternmost basin, Kotlujokull (Ko sector), is the largest and drains to the to the east (60 km^2), the Solheimajokull basin (So sector, 19 km^2) drains to the south, and the Entujokull basin (En sector, 23 km^2) to the northwest [1]. In historical times most floods have followed route Ko, a few have followed route So, whereas none have escaped through route En. Based on the eruption and jokulhlaup history, probabilistic models of eruption frequency for these basins can be constructed. Moreover, history also provides indications of eruption and jokulhlaup magnitude and how these parameters are related to the length of the interval between eruptions. In this article, we explore the relationship of these parameters using the probabilistic model, analysing spatial and temporal eruption patterns with the help of a Markov matrix in a similar way as used by Cronin et al. [6]. Previous attempts to analyse temporal eruption patterns of Icelandic volcanoes include the work of Thorarinsson [7], Wickman [8], Thorlaksson [9], Sigvaldason [10] and Gudmundsson and Saemundsson [11].

Additional information about the state of Katla volcano comes from geophysical monitoring. The volcano has been showing signs of unrest since 1999 when a shallow intrusion or a minor subglacial eruption occurred [12]. Elevated earthquake activity, increased geothermal activity, and several cm/year inflation of the caldera since then

suggest increasing pressure under the volcano [13]. These geophysical signals that suggest the volcano is near the end of a non-eruptive period are not considered in the study conducted here, which is based on purely statistical analysis of the eruption history.

2. Historical eruptions and jokulhlaups

Old documents, such as annals and records privately kept by farmers and clergymen, and official records kept by the local sheriffs [14–16], contain the eruption dates and descriptions of 14 Katla historical eruptions and the associated jokulhlaups [3]. Mapping of tephra deposits around Myrdalsjokull has added six further Katla eruptions and a major eruption in the associated and partly subglacial Eldgja fissure, raising the number of eruptions to 21 in historical time [4]. In table 1, historical eruptions are summarized [3, 4] together with 8th and 9th century Solheimajokull jokulhlaups/eruptions [17].

Table 1
Eruptions that have broken through the ice in the Katla caldera since the 8th century A.D.

Location of flood	Time of event	Eruption starts	Interval before	Interval after	Tephra layers	Magnitude of flood
Ko	1918	Oct. 12	58	(86+)	Large	Large
Ko + (So)	1860	May 8	37	58	Small	Small
Ko	1823	Jun. 26	68	37	Small	Medium
Ko	1755	Oct. 17	34	68	Large	Large
Ko	1721	May 11	61	34	Medium	Large
Ko	1660	Nov. 3	35	61	Medium	Med/Large
Ko	1625	Sept. 2	13	35	Large	Medium
Ko	1612	Oct. 12	32	13	Small	Small
Ko	1580	Aug. 11	80	32	Small	Small/Med
Ko	1500		(20)	80	Large	Med/Large
Ko	15th century		(20)	(20)	Small	?
Ko	1440		(24)	(20)	Small	?
Ko	1416		(59)	(24)	Medium	?
Ko	1357		(95)	(59)	Medium	?
Ko	1262		17	(95)	Large	?
Ko	1245		(66)	17	Small	?
Ko	1179		(50)	(66)	Small	?
Ko	12 century		(200)	(50)	Small	?
Ko, So[a]	934/938		(16)	(200)	Large	Very large
Ko	920		(20)	(16)	Medium	?
Ko	9th century		–	(20)	Small	?
So	9th century		–	–	Small	?
So	8th century		–	–	Medium	?

[a]Eldgja eruption, an event that was exceptional in magnitude and location of eruption.

These eruptions produced airborne tephra that allow an estimate of a minimum volume of the magma erupted. However, a large part of the material erupted in each Katla eruption is transported by jokulhlaups down to the sandur plains. Such events lead to the floods (jokulhlaup is Icelandic for glacial bursts) when the meltwater forces its way under the ice sheet and releases an immense flood on the waterway of the glacial river downstream of the glacier itself [3, 4, 15]. Water discharge in such floods may be 2 or 3 orders-of-magnitude greater than the natural floods occurring at interval of 5–10 years. They are therefore life-threatening events for the local population in the floodplains of the glacial rivers [5].

The extremely high meltwater production and melting rates observed in some subglacial eruptions has been attributed to extensive magma fragmentation. The degree of fragmentation observed in phreatomagmatic eruptions is such that thermal equilibrium times between magma and meltwater is of the order of seconds [18, 19]. The resulting heat transfer rates are considered to be the main reason for the magnitude of the Katla jokulhlaups.

3. Prehistoric eruptions and jokulhlaups

Tephra deposits in soils in the vicinity of Myrdalsjokull manifest that eruptions have occurred within the Katla caldera since ca. 6500 B.C. with similar or somewhat higher eruption frequency than that of the past millennium [20]. Most of these eruptions took place within the Ko sector. The occurrence of eruptions within the So sector and resulting jokulhlaups is based on geological evidence together with vague references to floods in old scripts [3, 4]. There are only geological records of jokulhlaups from the En sector [21–25]. These floods emit from Entujokull in the northwest corner of the caldera. Smith [23] and Larsen et al. [25] identify at least 10 large and medium En-type jokulhlaups in the last 8,000 years, suggesting a recurrence time of 500–800 years.

4. Eruption magnitude and flood magnitude

Extensive fieldwork has been carried out to map the distribution and thickness of historical Katla tephra layers, including the tephra layer of the last Katla eruption to break through the ice in 1918 [3, 4, 17, 26] (Larsen, unpublished data). Although this is a work in progress, results obtained so far allow the volume of airborne tephra in these eruptions to be grouped into four categories: small, volume <0.1 km^3; medium, volume between 0.1 and 0.5 km^3; large, volume between 0.5 and 1.5 km^3; very large, volume >1.5 km^3 (table 1). This classification covers only the airborne part of the total erupted material; the water-transported part is not taken into account. Presumably, the water-transported part represents, to a large extent, material erupted subglacially, mainly during the fully subglacial phase of an eruption, when it is

melting its way through the glacier in the first few hours of an eruption. The volume of this material may vary considerably, but it is reasonable to assume that it is related to eruption rate and ice thickness, which is 400–600 m in most parts of the caldera. The volume of this water-transported part should therefore correlate positively with the volume of airborne tephra in each eruption. We therefore regard the volume classification in table 1 as a useful qualitative comparison of the magnitudes of historical Katla eruptions. As shown in figure 3, some correlation exists between eruption magnitude and the following eruption interval (correlation coefficient of 58%). The Eldgja fires of 934 stand out as a special case. The total magma volume erupted in this event was some 19 km^3, including 5 km^3 of airborne tephra. It was therefore an order-of-magnitude larger than any of the eruptions that have occurred since then [4]. To be consistent with figures, it would have to be 4 times larger than the 'large' category. However, it was emitted from a fissure extending to the north through the caldera rim, so a large part of the tephra and all the lava was emitted outside the caldera. This event is therefore not included in figure 3.

A glacial flood from Katla consists of water, ice and volcanic debris, the proportions of which may vary between eruptions and also along the flood route in each flood. The water component of the floods is the water that the eruption melts out of the ice cap, and therefore one expects a certain relationship between the magnitude of the eruption and the magnitude of the flood volume. Therefore, the correlation between flood volumes and eruption magnitude has to be investigated. Tomasson [5] estimated the flood water volume of the 1918 jokulhlaup as 8 km^3, and the peak flow rate as 300,000 m^3/s. This was one of the largest Katla floods. Several of the written records of older eruptions [14–16] contain descriptions of which areas were affected by the associated floods. This allows the probable magnitude of the associated floods to be estimated by comparing them to the large 1918 jokulhlaup. In table 1, the

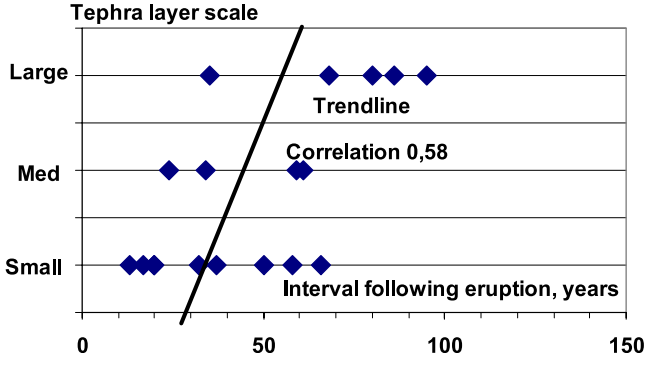

Figure 3. Correlation of interval between eruptions and eruption magnitude. Correlation is assigned using the following values: small = 1, medium = 2, large = 3 (excluding the Eldgja eruption which was of exceptional magnitude).

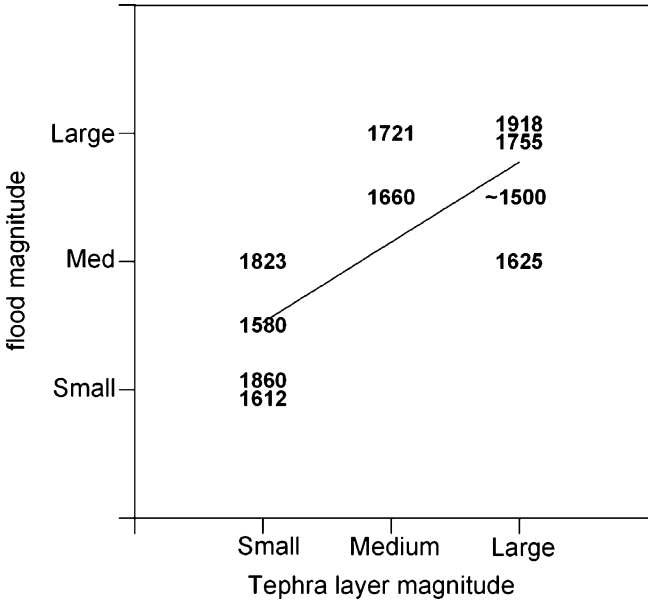

Figure 4. The relationship between eruption magnitude and jokulhlaup magnitude after 1500 A.D. Eruption years and magnitudes are as in table 1. A quantitative correlation coefficient of 0.75 of the line shown is obtained by assigning numbers to the descriptive magnitudes: small = 1, small/med = 1.5, medium = 2, med/large = 2.5, large = 3.

relative magnitude of the floods after 1500 A.D. has, accordingly, been grouped into small, medium and large on the basis of documentary evidence. The data is rather uncertain and by no means as comprehensive as the data for the tephra emissions (table 1). However, as figure 4 shows, a correlation exists between eruption magnitude and jokulhlaup magnitude, as expected.

5. Probabilistic model of eruption distribution and frequency

5.1. Choice of a probabilistic model

The main hazard in eruptions of Katla volcano is due to the jokulhlaups. Thus, the magnitude of jokulhlaups and their recurrence times are the most important parameters to obtain in hazard assessment. However, jokulhlaup volumes are poorly quantified. In comparison, the record of eruption magnitudes, crude as it may be, is much better constrained. We therefore proceed by exploring the properties of the eruption history through a probabilistic model.

In the following we only consider eruptions that cause substantial jokulhlaups, melt their way through the glacier and produce tephra layers. These types of events are registered in the eruption history in table 1. A probabilistic model for the year X_i when

such eruptions occur can, in general terms, be formulated from the year of the last eruption X_{i-1} as:

$$X_i = X_{i-1} + \xi_i \tag{1}$$

Here, ξ_i is a stochastic random variable that takes one value for every i and indicates the time between eruptions. It remains to be determined in which sector the eruption occurs: Ko, So or En.

Before proceeding further, a choice has to be made between two different models for volcanism in the caldera:

(a) Eruptions in all three sectors are independent events.

(b) Eruptions within the caldera are stochastically related events.

Current data in the eruption history (table 1) does not hold enough information to choose between these mutually exclusive lemmas. It is quite clear that eruptions within the Ko sector are more frequent than in the other sectors, but this can be reconciled with both (a) and (b). If item (a) is true, then average intervals between eruptions are an order-of-magnitude shorter in Ko than in the other sectors. If item (b) is true, eruption activity jumps between sectors with a much larger probability of hitting Ko than the other sectors. The average interval between eruptions is a parameter that should describe the whole caldera, taking into account eruptions at all locations considered.

The choice between (a) and (b) therefore has to be made upon geophysical and geological evidence rather than mathematical manipulations of the data in table 1. It is important to realize that the boundaries of the three sectors (Ko, So and En) are controlled by the ice surface topography, and not by structural boundaries within the volcano; they all belong to the same caldera [1]. Seismic undershooting has revealed a shallow magma chamber in the northeastern part of the caldera (northern part of sector Ko) [27]. Other geophysical data such as distribution of seismicity and geothermal activity, inflation of the caldera in recent years, and magnetic and gravity anomalies indicate the absence of other structural units comparable to the magma chamber within the caldera itself [12, 28–30]. This evidence indicates that tectonic activity within the caldera is related, but not independent, in all three sectors. It is therefore assumed that lemma (b) is more likely to describe the volcanic activity correctly.

Considerable literature exists on eruption statistics. Most studies have concentrated on temporal variations in eruption occurrence and/or magnitude. Bebbington and Lai [31] used renewal models to analyse records for the volcanoes Ruapeu and Ngauruhoe. Marzocchi et al. [32] proposed an event tree model, assigned probabilities to various scenarios and applied the model to Vesuvius. Spatial distribution of volcanic vents was taken into account by Connor and Hill [33] in their analysis of probability of eruptions within the Yucca Mountain region, Nevada, by using

nonhomogeneous Poisson models. Cronin et al. [6] used a Markov matrix to perform a spatial and temporal analysis on the recurrence rate of eruptions on individual segments of the Taveuni volcano, Fiji. In this work, we adopt a similar approach and assume that our time series of volcanic eruptions classifies as a Markov chain, and that migration of activity from one part of the Katla caldera to another may be described by a stochastic Markov matrix. Below, a stochastic model is constructed and its parameters tested on the data in table 1.

5.2. *The probability of an eruption in a given location*

Let a major eruption hit one of the three sectors (Ko, So, En), thereby causing a large flood. The next eruption can hit any of the three sectors. A Markov matrix gives the probabilities that the eruption will hit a new location or stay at the same one. In our case it is a 3 × 3 probability matrix $p_{n,m}$; n and m will take the values 1, 2, 3, governing where the next eruption will hit. In the following, if we let n or m be equal to 1, it implies eruption in sector Ko, 2 implies So, and 3 implies En. As an example, $p_{1,3}$ will, in this terminology, be the probability that the next eruption takes place in sector En (=3), provided the last one took place in sector Ko (Katla flood = 1). By definition, we will have

$$\sum_{m=1}^{m=3} p_{n,m} = 1 \text{ for any } n \tag{2}$$

This probability model is in accordance with lemma (b). With this choice of model simultaneous eruptions at two different locations are excluded. This is not strictly in accordance with the eruption history, but such events are rare and we regard this as a justifiable simplification.

5.3. *The eruption series X_i*

The interval between any two eruptions, denoted by ξ_i, in equation (1), can be written as

$$\xi_i = m_y + s_y \eta_i(0,1) \tag{3}$$

Here, m_y and s_y are the mean value and standard deviation of the intervals in years between eruptions in the caldera compiled from table 1. η_i is a stochastic variable with mean 0 and standard deviation 1, taking one value for each i. The frequency distribution on η_i and the intervals in years between eruptions must be the same. Equation (3) will be used for simulation of time intervals between eruptions. Eruption probabilities can now be simulated using equations (1)–(3). Figure 5 shows a comparison between the intervals between the first 20 eruptions in table 1 and a

lognormal distribution. The fit is quite reasonable and we consider it sufficiently good to warrant the use of a modified version of equation (3) in our calculations:

$$\xi_i = \exp\left(m_y + s_y \eta_i(0,1)\right) \tag{4}$$

Now m_y is the average of the logarithms ($\log_e$) of the time intervals in table 1, and s_y is the standard deviation of the logarithms ($\log_e$) of the time intervals in table 1. This equation will be used in the simulation and then the number of eruptions can be counted and probabilities calculated.

5.4. *The location series Y_i*

We define a location series Y_j alongside with the eruption series. The location series can only take three values, 1, 2 or 3, with Ko => $Y_j = 1$, So => $Y_j = 2$ and En => $Y_j = 3$. Now recall the probability matrix (equation (2)). If we denote the last eruption by Y_{j-1}, the value of this variable will be the number n in the probability matrix $p_{n,m}$. The probability matrix is rewritten as a new matrix P for mathematical convenience. The first line in the P matrix is:

$$P_{1,m} = \left\{1; p_{1,2} + p_{1,3}; p_{1,3}\right\} \text{ for } Y_{j-1} = 1 \tag{5}$$

This first line corresponds to $Y_{j-1} = 1$ indicating that last eruption was in the Ko sector. Lines 2 and 3 in the P matrix correspond similarly to $Y_{j-1} = 2$ and 3. In order to control the migration of next eruption between the sectors Ko, So, and En, we now define $0 < \theta_j < 1$ as a new evenly distributed random variable taking one value for

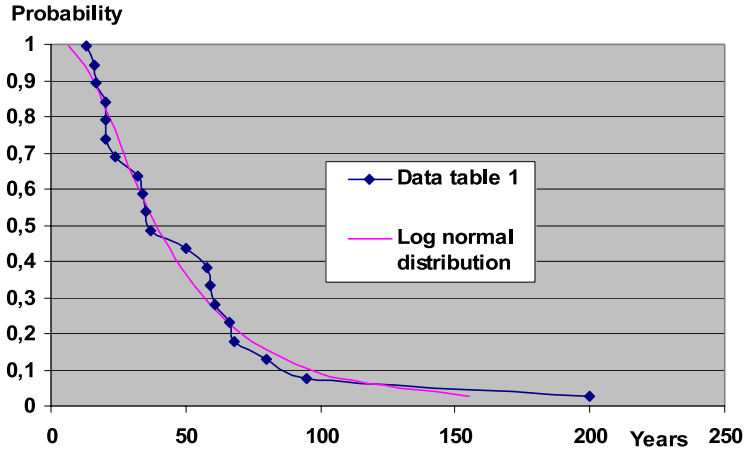

Figure 5. Distribution of time intervals between eruptions within the Katla caldera (all sectors).

each j. With eruption $j - 1$ taking place in location $Y_{j-1} = 1$, the next eruption will take place in $Y_j = 1$, 2 or 3. The exact value will be

$$\begin{aligned} Y_j &= 1 \text{ for } \theta_j > P_{1,2} = p_{1,2} + p_{1,3} \\ Y_j &= 2 \text{ for } P_{1,2} > \theta_j > P_{1,3} = p_{1,3} \\ Y_j &= 3 \text{ for } \theta_j \leq P_{1,3} = p_{1,3} \end{aligned} \tag{6}$$

Similar rules apply for $Y_{j-1} = 2$ and 3. Having found Y_j, Y_{j+1} can readily be found. In this manner of successive calculation, a time series can be constructed. Provided the probabilities in equation (6) are known, eruption histories long enough to determine probabilities of rare events can be simulated. There are six (3×2) P_m values, corresponding to the probability matrix $p_{n,m}$, that have to be selected.

5.5. *Parameters of the simulation*

Based on the data covering the period 1200–1300 in table 1, the average interval between eruptions is 52–57 years. We are confident that the record is complete for the last 500 years, but cannot exclude the possibility of gaps prior to 1500 A.D. Thus, we use the last 500 years to define a mean eruption interval of 49 years and a standard deviation of 25 years as key parameters in the simulation. These parameters are in reasonable agreement with the longer record although a standard deviation cannot be reliably determined due to large uncertainties in some of the pre-1500 A.D. eruption dates.

The Markov matrix (equation (2)) has to be selected. The only possibility to do so is to conclude that the eruption history in table 1 has a high probability. After several runs and subsequent adjustments, a good fit was obtained, incorporating all known information (table 1 and the geological data on So and En eruptions). This matrix is given in table 2a.

The probabilities of the eruption "jumping" between the three regions is implicit in the Markov matrix. For example, if the last eruption was in Ko, and the number in the So column is 0.11, then there is a probability of $(1 - 0.11) \times 100 = 89\%$ that the

Table 2a
Markov matrix set 1.

		Ko = 1	So = 2	En = 3
Three runs done				
Last eruption	Ko = 1	1	0.11	0.07
	So = 2	1	0.45	0.07
	En = 3	1	0.3	0.07

Table 2b
Markov matrixes for three runs.

		Ko = 1	So = 2	En = 3
Run 1				
Last eruption	Ko = 1	1	0.1	0.035
	So = 2	1	0.4	0.035
	En = 3	1	0.4	0.035
Run 2				
Last eruption	Ko = 1	1	0.15	0.035
	So = 2	1	0.15	0.035
	En = 3	1	0.15	0.035
Run 3				
Last eruption	Ko = 1	1	0.1	0.04
	So = 2	1	0.4	0.01
	En = 3	1	0.4	0.01

next eruption will take place in Ko. If there is 0.07 in the En column, there is a (0.11 − 0.07) × 100 = 4% probability the next eruption will occur in So and a 7% probability that it will be in En.

To test the robustness of the simulation procedure, three runs were performed for the Markov matrix in table 2a. In addition, three other matrixes were tested by varying slightly the probabilities and the jumping tendency (table 2b). However, the relative dominance of the Ko sector was not significantly altered, because it is one of the strongest characteristics of the data. For all practical purposes, results are similar for all runs – indicating that the procedure is stable.

6. Simulation results

Simulation was performed using a Monte Carlo operator in a spreadsheet program. To obtain a stable solution, we used a simulation period that is much longer than the duration of any semi-regular state of the volcano. Hence, a simulation period of ~570,000 years was used, equivalent to summing the results of 475 simulations of eruption probabilities over the next 1,200 years. However, the results do not provide a description of the long-term future behaviour nor the pre-Holocene behaviour of the volcano.

The results (table 3a and b) give time intervals between eruptions in the three sectors.

Table 3a shows that the three runs in set 1 are almost identical, revealing that model errors are small, the simulation period long enough and runs can be repeated. Comparison with table 3b shows that the So and En eruption probabilities change only slightly, when changes that keep the Ko probabilities constant are made on the Markov matrix.

Table 3a
Results of simulation over 569,365 years, set 1.

	Run	Ko	So	En
Number of eruptions	1	9,862	952	830
	2	9,862	952	830
	3	9,919	917	808
Average time interval (years)	1	58	601	689
	2	58	601	689
	3	57	621	705
Most probable t.i. (years)	1	33	49	140
	2	33	51	145
	3	38	51	145
Largest time interval (years)	All	568	7,087	4,705
Average between eruptions in caldera			All	49

Table 3b
Results of simulation over 566,925 years, set 2.

	Run	Ko	So	En
Number of eruptions	1	9,951	1,277	416
	2	9,880	1,308	456
	3	9,980	1,255	409
Average time interval (years)	1	57	448	1,375
	2	58	441	1,266
	3	57	452	1,387
Most probable t.i. (years)	1	34	43	150
	2	33	50	100
	3	34	45	200
Largest time interval (years)	All	539	5,453	12,143
Average between eruptions in caldera			All	49

The average time intervals between eruptions are in good accordance with expectations. The most probable intervals are surprisingly low, and the largest intervals produced are also quite long. The longest simulated intervals do not have a statistical significance. However, they demonstrate that intervals of several hundred years for the Ko sector and several thousand years for the So and En sectors have non-zero probabilities.

The probability density functions (pdf) for simulations in table 2a (set 1) are presented in figure 6a–c. The Ko pdf has all the characteristics one would expect. The most probable time interval is a little lower than the average interval and long time intervals are rare. The So probability density function is markedly different from that of Ko pdf. The maximum (most probable time interval) is higher than for the Ko pdf. The So pdf is a little narrower, but the tail is much longer. This suggests that an

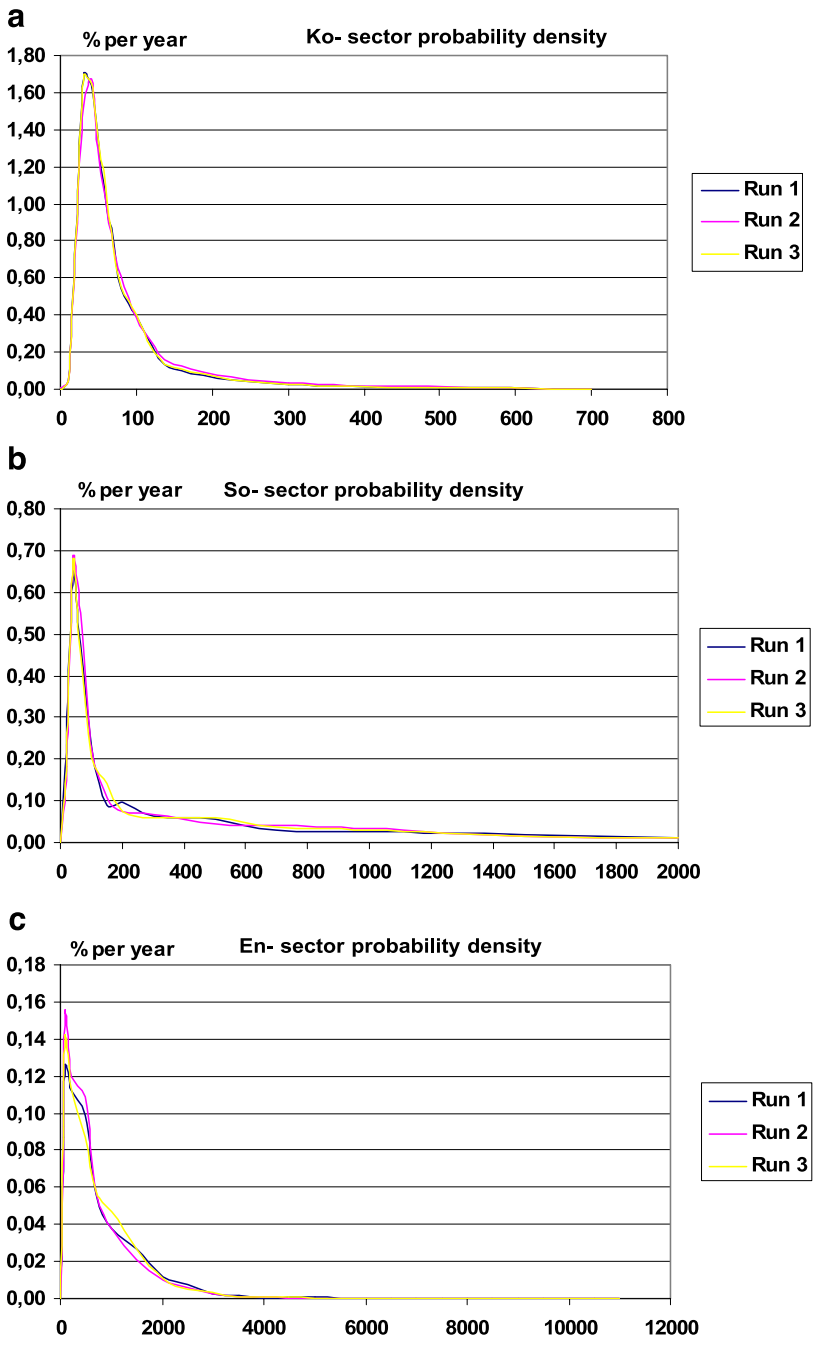

Figure 6. Probability density functions for eruptions. (a) Ko sector, (b) So sector, (c) En sector.

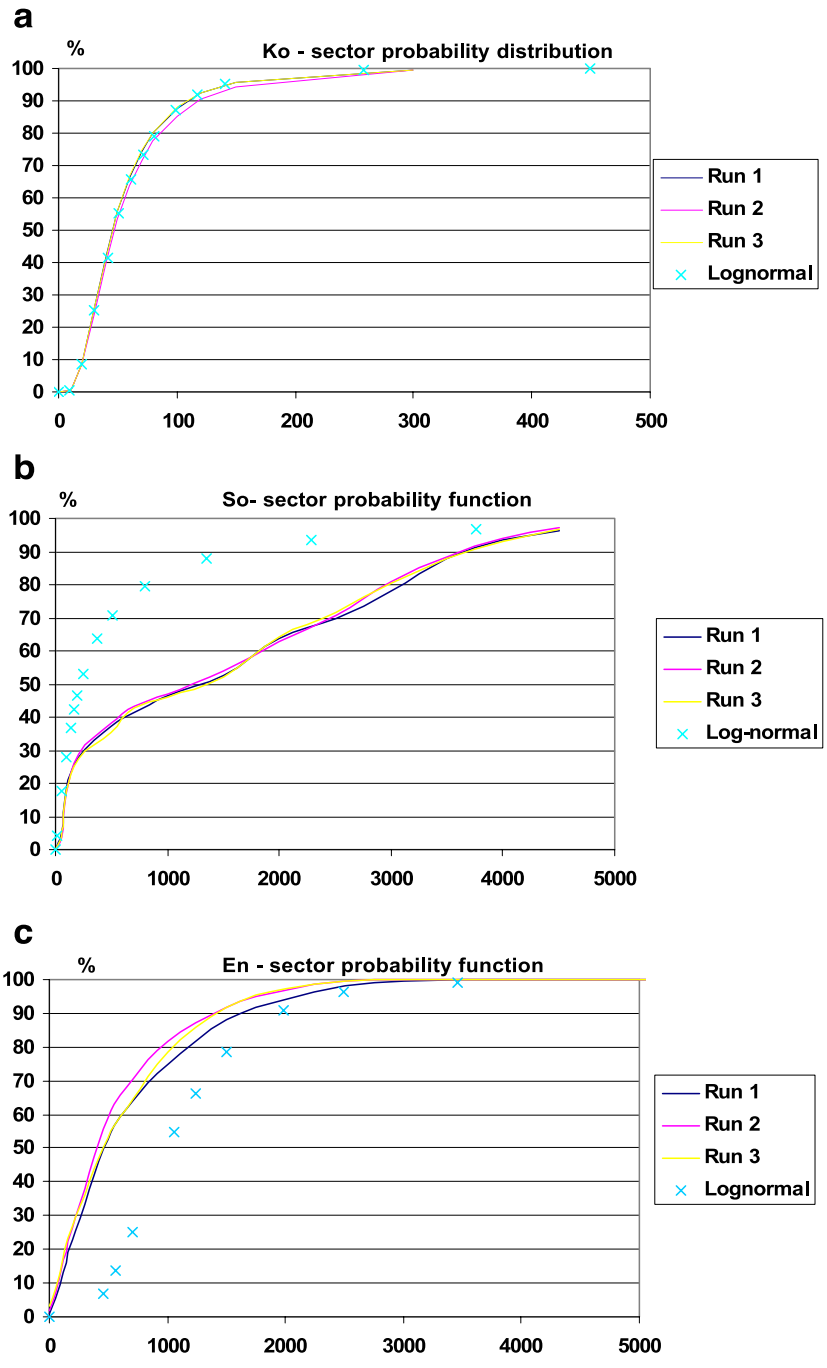

Figure 7. Probability distribution function of time intervals between eruptions compared to a lognormal distribution. (a) Ko sector, (b) So sector, (c) En sector.

eruption within the So sector is rather likely to be followed by another eruption within that sector. These features are even more prominent in the En pdf. In general, however, we have the same characteristics here as for the So sector. An eruption within the En sector is rather likely to be followed by another eruption within that sector. As expected, model errors are greater in pdf of En and So than in the Ko pdf. However, the maximum density for En and So is stable for all simulations.

In order to check (validate is to strong a word here) the choice of model discussed in section 5.1, the distribution functions of set 1 were calculated (figure 7) and compared to the lognormal distribution. If model (a) in section 5.1 had been chosen, all eruption intervals in all locations would be distributed according to the lognormal distribution. The distributions were calculated for the average values (table 3a, b) and standard deviations for all three runs in each location.

For the Ko sector the distribution function followed the lognormal very closely (Figure 7a). Simulation results give slightly lower probabilities for intervals less than 150 years than the lognormal, but the difference is insignificant since such long eruption intervals are very rare in table 1. One must bear in mind, however, that the average eruption interval resulting from the simulations (table 3a) is 58 years, but model (a) would give 49 years as table 1 does. This difference, which is the result of the Markov matrix set 1, is significant.

In the So sector the distribution function is very different from the lognormal, (figure 7b). Here, the effect of the Markov model is clearly to distribute the probabilities of intervals of 100–5,000 years much more evenly than the lognormal distribution. Thus long intervals between eruption in the So location would be rare if the (a) model in section 5.1 had been chosen. Such behaviour is in contrast to present history (table 1), as there are no known eruptions in the So sector for more than 1,000 years. This supports the (b) model but cannot be taken as a proof.

In sector En the distribution function followed the lognormal not as closely as in the Ko sector but without significant differences. The main difference is that probabilities of long intervals (less than 2,000 years) are larger in the simulation results than in the lognormal case. This difference in models (a) and (b) in section 5.1 for sector En is the reverse of the difference in models for sector Ko. This result is supported by the fact that all 10 identified En eruptions have intervals of less than 2,000 years (see section 3).

7. Discussion

The correlation between the eruption interval and the magnitude of the preceding eruption (figure 3) is not strong, but it suggests that a long eruption interval has a tendency to follow a large eruption. No significant correlation exists between the magnitude of eruption and the length of the preceding eruption interval. The significance of this is somewhat unclear. If it is assumed that magma in Katla

eruptions comes from the shallow magma chamber in the northeastern part of the caldera [27], the correlation may imply that eruption magnitude is more dependent on the effectiveness of initial magma chamber rupturing than on variations between eruptions in initial magma chamber pressure or state of inflation. When an effective pathway for magma from the chamber is established, a large eruption occurs as it taps more magma from the chamber than would happen during the formation of a less effective pathway. When small amounts of magma are released from the chamber, recovery time is relatively short, but long when larger amounts are released. This notion remains speculative. However, if the indicated correlation is real, no inferences can be made about the magnitude of the next Katla eruption on the basis of the unusually long period since the last eruption (87 years).

Many volcanoes go through long episodes during their lifetime where activity is semi-regular. During these episodes the production rate remains similar for extended periods and they have a reasonably well-defined eruption frequency [34]. In addition, periods occur when eruptions mainly take place in one part of volcano, while other areas are mostly dormant (e.g., [33]). Then activity may occasionally jump from one part of the volcano to another. There are indications in the eruption history of Katla (table 1) that the So sector went through such a phase in the 8th–10th century. The pdf from the Markov simulations (figure 6) can be understood in terms of such episodes of migrating eruptive activity. The pdf for the So and En sectors are characterized by a relatively long average eruption interval when compared to the average for the caldera as a whole. This implies that in the event of activity moving from sector Ko to either So or En, the likelihood of a cluster of eruptions occurring in So or En is greatly increased. In theory, a clustering tendency could be more fully analysed by setting up a two-state model for each sector, with different eruption probabilities for "dormant" periods and active periods. However, our data are not sufficient to constrain any parameters of such a model. Further work on eruption history may make such an approach feasible in the future.

This clustering tendency has implications for the jokulhlaup hazard. In the absence of geophysical evidence that implies migration of magmatic activity to the So or En sectors, the probability of eruptions in these sectors in the near future remains low. On the other hand, if an eruption were to occur in the So or En sectors causing a jokulhlaup down to either Jokulsa a Solheimasandi or Markarfljot, there are increased chances of the next jokulhlaup following the same path. This possibility of clustering needs to be taken into account when plans are made for land use in the lowland areas that may be affected by So or En sector jokulhlaups.

The eruptions are not independent but have the dependence specified by the Markov matrix (table 2a). As the last eruption was an eruption in the Ko sector, the probability should be 89% for another eruption there, 4% for an eruption in the So sector, and 7% for an eruption in the En sector.

The last eruption in 1918 was large so the interval until the system erupts next time should also be large as figure 3 indicates. The average interval after the large

eruptions in table 1 is 73 years, excluding the exceptional Eldgja eruption. If the Eldgja eruption is included, the average interval after a large eruption becomes 95 years. Thus, its inclusion in the record does not drastically alter the results.

To calculate the internal statistics after a large event like 1918, we used the following equation of a simple single-variable linear-regression Gaussian stochastic process [35]:

$$\psi = m_\psi + r_{\xi\psi}(\xi - m_\xi)s_\psi/s_\xi + \sqrt{\left(1 - r_{\xi\psi}^2\right)s_\psi}\eta(0,1) \tag{7}$$

ψ	Magnitude of eruption
ξ	Length of interval (see equation (3))
m_ψ	Mean value of magnitude indicator (small = 1, med = 2, large = 3)
$r_{\xi\psi}$	Correlation between magnitude and interval length (0.58; see figure 3)
m_ξ	Mean interval used in the simulations
s_ψ/s_ξ	Standard deviation
$\eta(0,1)$	Gaussian distributed random variable as before

The results of simulations of intervals following a large eruption are shown in figure 8. The resulting probability function follows the lognormal distribution approximately, but there are deviations. The average interval is 73 years as indicated in table 1.

The probability of a new eruption in the near future is calculated from the tail distribution of the curve in figure 8. The probability, excluding the effect of the Eldgja event, is obtained using the curve marked as "NEXT73" in figure 9. The probability of an eruption within 50 years would be 72%, 50% within 29 years, and 20% within 10 years. If the Eldgjá event is included, the "NEXT95" curve on in figure 9 should be

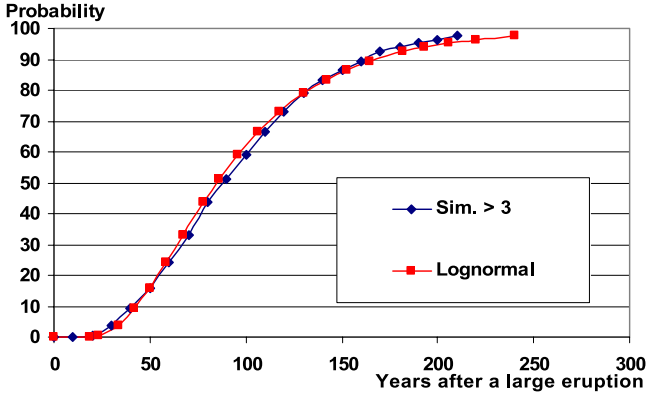

Figure 8. Simulation of intervals following large eruptions compared to a lognormal distribution.

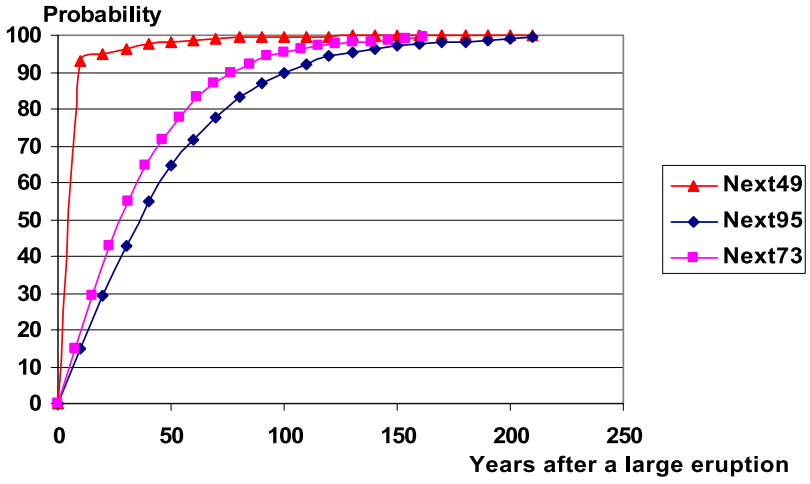

Figure 9. Probabilities of having an eruption after 2004, considering that a large eruption occurred in 1918. Three curves are shown. One for an average interval of 73 years (figure 8), one with the 95 years average interval (including Eldgja) and one using the magnitude-independent average (49 years).

used; results indicate a 65% probability of an eruption within next 50 years, 50% within 37 years, and 15% within the next 10 years. These two simulations can be compared to the result if no correlation is assumed between eruption magnitude and the following interval (marked as "NEXT49"). Then there would be a 93% probability of an eruption within the next 10 years.

It must be stressed that ice cauldron formation, earthquakes, inflation of the caldera and other activity observed in the Katla volcanic system may give indications of the next eruption that are not included in the probabilities reported here. The above probabilities may therefore be regarded as minimum values and are subject to revision if new evidence is brought forward by ongoing research.

Our model clearly shows that the probabilities of eruptions in all sectors of the caldera are significant despite the dominance of the Ko sector. This demonstrates the need of geophysical monitoring of the whole Katla volcano if plausible warnings of future eruptions are to be issued.

8. Conclusion

The Katla caldera is divided into three sectors, defined by the areas from which jokulhlaups will escape through the Kotlujokull pass (the Ko sector), the Solheima-jokull pass (the So sector) and Entujokull (the En sector). Eruption frequency differs in the three sectors but eruption activity is considered to migrate between the sectors. On the basis of eruption and jokulhlaup history, the average time interval between eruptions inside the caldera (all sectors) is calculated as 49 years. Eruptions are most common in the Ko sector with the average long-term eruption interval considered to

be 58 years. The average time interval between eruptions is considered to be approximately 600 years in the So sector and approximately 500–800 years in the En sector.

A positive correlation exists between eruption magnitude and length of the following interval in years. Inferences about the magnitude of the next Katla eruption therefore cannot be made on grounds of the length of the preceding interval. Jokulhlaup magnitude is positively correlated with eruption magnitude in the Ko sector. Such correlation is likely to exist for the others sectors as well. Together, these two correlations yield a weak correlation between jokulhlaup magnitude and length of the following eruption interval. The effect of this correlation on jokulhlaup statistics has to be further investigated.

Our statistical approach suggests there is an 89% probability that the next eruption occurs within the Ko sector, a 4% probability that it occurs within the So sector, and a 7% probability within the En sector.

Two possible stochastic models were considered: one model with independent eruption activity in all three sectors and another with the eruption activity migrating between the sectors according to a Markov probability matrix. The eruption time series has been simulated by a Markov process, as these results were better supported by the history of volcanic activity known from historical and geological records. The simulations predict that the most probable eruption interval for the En sector and the So sector is an order-of-magnitude smaller than the average time interval. This can be understood as infrequent periods when eruptions occur at short intervals in the En and So sectors, during which the otherwise dominant Ko sector may be resting. This prediction is supported by the eruption history of the So sector during the last 1,300 years.

The most probable time intervals between eruptions in the three sectors are greatly influenced by the correlation between interval length and eruption magnitude. The average interval after a large eruption like 1918 is 73 years, making the probability of a new eruption in the Katla caldera within 10 years after 2004 20% instead of 93% as would be the case if this correlation is not considered.

References

[1] H. Bjornsson, F. Palsson and M.T. Gudmundsson, Surface and bedrock topography of the Myrdalsjokull ice cap, Iceland, Jokull 49 (2000) 29–46.
[2] S. Rist, *Vatns er thorf* [Water is a need] (Menningarsjodur, Reykjavik, 1990) 248 pp.
[3] S. Thorarinsson, Katla og annall Kotlugosa [Katla volcano and annals of Katla eruptions], Arbok Ferdafelags Islands (1975) 125–149.
[4] G. Larsen, Holocene eruptions within the Katla volcanic system, south Iceland: characteristics and environmental impact, Jokull 49 (2000) 1–28.
[5] H. Tomasson, The jokulhlaup from Katla in 1918, Ann. Glaciol. 22 (1996) 249–254.
[6] S.J. Cronin, M. Bebbington and C.D. Lai, A probabilistic assessment of eruption recurrence on Taveuni volcano, Fiji, Bull. Volcanol. 63 (2001) 274–288.
[7] S. Thorarinsson, On the predicting of volcanic eruptions in Iceland, Bull. Volcanol. XXIII (1960) 45–53.

[8] F.E. Wickman, Repose-period patterns of volcanoes. IV. Eruption histories of some selected volcanoes, Ark. Mineral. Geol. 4 (1966) 337–350.
[9] J.E. Thorlaksson, A probability model of volcanoes and the probability of Eruptions of Hekla and Katla, Bull. Volcanol. XXXI (1967) 97–106.
[10] G.E. Sigvaldason, Volcanic prediction in Iceland, NVI Research Report 7902, Nordic Volcaological Institute, Reykjavik (1979) 26 p.
[11] G. Gudmundsson and K. Saemundsson, Statistical analysis of damaging earthquakes and volcanic eruptions in Iceland from 1550–1978, J. Geophys. 47 (1980) 99–109.
[12] E. Sturkell, F. Sigmundsson and P. Einarsson, Recent unrest and magma movements at Eyjafjallajokull and Katla volcanoes, Iceland, J. Geophys. Res. 108(B8) (2003) 2369, doi: 10.1029/2001JB000917.
[13] E. Sturkell, P. Einarsson, F. Sigmundsson, H. Geirsson, H. Olafsson, R. Olafsdottir and G.B. Gudmundsson, Thrystingur vex undir Kotlu [Increasing magma pressure under Katla], Natturufraedingurinn 71 (2003) 80–86.
[14] Skyrslur um Kotlugos [Reports on the eruptions of Katla], *Safn til sögu Íslands IV*, (Hid Islenzka Bokmenntafelag, Kaupmannahofn og Reykjavik, 1907–1915) pp. 186–294.
[15] G. Sveinsson, *Kotlugosid 1918 og afleidingar thess* [The 1918 Eruption of Katla and Its Consequences] (Prentsmidjan Gutenberg, Reykjavik, 1919) 61 pp.
[16] G. Johannson, *Kotlugosid 1918* [The Katla Eruption of 1918], (Prentsmidjan Gutenberg, Reykjavik, 1919) 70 pp.
[17] G. Larsen, *Gjoskulog i nagrenni Kotlu* [Tephra Layers in the Vicinity of Katla], B.Sc. hons. thesis, University of Iceland, Reykjavik (1978) 57 pp.
[18] M.T. Gudmundsson, Melting of ice by magma–ice–water interactions during subglacial eruptions as an indicator of heat transfer in subaqueous eruptions, in: Explosive Subaqueous Volcanism, Geophysical Monograph 140, eds. J.D.L. White, J.L. Smellie and D. Clague (American Geophysical Union, 2003) pp. 61–72.
[19] M.T. Gudmundsson, F. Sigmundsson, H. Bjornsson and Th. Hognadottir, The 1996 eruption at Gjalp, Vatnajokull ice cap, Iceland: efficiency of heat transfer, ice deformation and subglacial water pressure, Bull. Volcanol. 66 (2004) 46–65.
[20] B.A. Oladottir, Eruption history and magmatic evolution at the Katla volcanic system, Iceland, during the Holocene, DEA thesis, Universite Blaise Pascal, Clermont-Ferrand (2004).
[21] H. Haraldsson, The Markarfljot Sandur Area, Southern Iceland: Sedimentological, Petrographical and Stratigraphical studies, Ph.D. thesis (Uppsala University, Uppsala, 1981) 65 pp.
[22] F. Sigurdsson Fold og votn ad Fjallabaki [Rivers and range in the Fjallabak area], Arbok Ferdafelags Islands (1988) 181–202.
[23] K.T. Smith, A.J. Dugmore, G. Larsen, E.G. Vilmundardottir and H. Haraldsson, New evidence for Holocene jokulhlaup routes west of Myrdalsjokull, in: The 25 Nordic Geological Winter Meeting Abstracts volume, ed. S.S. Jonsson (Reykjavik, 2002) p. 196.
[24] I. Kaldal and E.G. Vilmundardottir, Jokulmenjar a Emstrum, nordvestan Myrdalsjokuls, Research Report OS-2002/080 (Orkustofnun, Reykjavik, 2002) 29 pp.
[25] G. Larsen, K. Smith, A.J. Newton and O. Knudsen, Jokulhlaup til vesturs fra Myrdalsjokli: Ummerki um forsoguleg hlaup nidur Markarfljot. [Jokulhlaups towards west from Myrdalsjokull: Prehistoric floods in Markarfljot river], in: *Hættumat vegna eldgosa og hlaupa frá vestanverðum Myrdalsjokli og Eyjafjallajokli* (Rikislogreglustjori, Reykjavik, 2005) pp. xx–yy (in Icelandic).
[26] S. Thorarinsson, Langleiðir gjosku ur Þremur Kotlugosum, Jokull 30 (1980) 65–73.
[27] O. Gudmundsson, B. Brandsdottir, W. Menke and G.E. Sigvaldason, The crustal magma chamber of the Katla volcano in south Iceland revealed by 2-D seimic undershooting, Geophys. J. Int. 119 (1994) 277–296.
[28] P. Einarsson and B. Brandsdottir, Earthquakes in the Myrdalsjokull area, Iceland, 1978–1985: seasonal correlation and connection with volcanoes, Jokull 49 (2000) 59–74.

[29] M.T. Gudmundsson, The structure of Katla, a central volcano in a propagating rift zone, south Iceland from gravity data, EOS Trans. AGU 75 (1994) 335.
[30] G. Jonsson and L. Kristjansson, Aeromagnetic measurements over Myrdalsjokull and vicinity, Jokull 49 (2000) 47–58.
[31] M.S. Bebbington and C.D. Lai, Statistical analysis of New Zealand volcanic occurrence data, J. Volcanol. Geotherm. Res. 74 (1996) 101–110.
[32] W. Marzocchi, L. Sandri, P. Gasparini, C. Newhall and E. Boschi, Quantifying probabilities of volcanic events: the example of volcanic hazard at Mount Vesuvius, J. Geophys. Res. 109 (2004) B11201.
[33] C.B. Connor and B.E. Hill, Three nonhomogeneous Poisson models for the probability of basaltic volcanism: application to the Yucca Mountain region, Nevada, J. Geophys. Res. 100 (1995) 10107–10125.
[34] G.P.L. Walker, Basaltic volcanoes and volcanic systems, in: *Encyclopedia of volcanoes*, ed. H. Sigurdsson (Academic Press, San Diego, 2000) 283–289.
[35] K.V. Mardia, J.T. Kent and J.M. Bibby, *Multivariate Analysis* (Academic Press, London, 1979).